

Journal of Coordination Chemistry

Publication details, including instructions for authors and subscription information:

<http://www.tandfonline.com/loi/gcoo20>

Synthesis and X-ray crystal structures of N,N,N',N'-tetraalkylpyridine-2,6-dithiocarboxamides (S-dapt) complexes of cobalt(II) and nickel(II)

Pratibha Kapoor^a, Ajay Pal Singh Pannu^b, Love Karan Rana^c,
Ramesh Kapoor^d, Geeta Hundal^c & Maninder Singh Hundal^c

^a Department of Chemistry, Panjab University, Chandigarh, India

^b Institute of Fundamental Sciences, Massey University,
Palmerston North, New Zealand

^c Guru Nanak Dev University, Amritsar, India

^d Department of Chemistry, Indian Institute of Science Education
and Research, Chandigarh, India

Accepted author version posted online: 29 Oct 2013. Published
online: 04 Dec 2013.

To cite this article: Pratibha Kapoor, Ajay Pal Singh Pannu, Love Karan Rana, Ramesh Kapoor, Geeta Hundal & Maninder Singh Hundal (2013) Synthesis and X-ray crystal structures of N,N,N',N'-tetraalkylpyridine-2,6-dithiocarboxamides (S-dapt) complexes of cobalt(II) and nickel(II), Journal of Coordination Chemistry, 66:23, 4144-4162, DOI: [10.1080/00958972.2013.859679](https://doi.org/10.1080/00958972.2013.859679)

To link to this article: <http://dx.doi.org/10.1080/00958972.2013.859679>

PLEASE SCROLL DOWN FOR ARTICLE

Taylor & Francis makes every effort to ensure the accuracy of all the information (the "Content") contained in the publications on our platform. However, Taylor & Francis, our agents, and our licensors make no representations or warranties whatsoever as to the accuracy, completeness, or suitability for any purpose of the Content. Any opinions and views expressed in this publication are the opinions and views of the authors, and are not the views of or endorsed by Taylor & Francis. The accuracy of the Content should not be relied upon and should be independently verified with primary sources of information. Taylor and Francis shall not be liable for any losses, actions, claims, proceedings, demands, costs, expenses, damages, and other liabilities whatsoever or howsoever caused arising directly or indirectly in connection with, in relation to or arising out of the use of the Content.

This article may be used for research, teaching, and private study purposes. Any substantial or systematic reproduction, redistribution, reselling, loan, sub-licensing, systematic supply, or distribution in any form to anyone is expressly forbidden. Terms & Conditions of access and use can be found at <http://www.tandfonline.com/page/terms-and-conditions>



Synthesis and X-ray crystal structures of N,N,N',N'-tetraalkylpyridine-2,6-dithiocarboxamides (S-dapt) complexes of cobalt(II) and nickel(II)

PRATIBHA KAPOOR[†], AJAY PAL SINGH PANNU[‡], LOVE KARAN RANA[§],
RAMESH KAPOOR[¶], GEETA HUNDAL[§] and MANINDER SINGH HUNDAL^{*§}

[†]Department of Chemistry, Panjab University, Chandigarh, India

[‡]Institute of Fundamental Sciences, Massey University, Palmerston North, New Zealand

[§]Guru Nanak Dev University, Amritsar, India

[¶]Department of Chemistry, Indian Institute of Science Education and Research, Chandigarh, India

(Received 7 June 2013; accepted 30 August 2013)

Reactions of anhydrous CoX_2 ($\text{X} = \text{Br}^-$, SCN^-) and $\text{Ni}(\text{ClO}_4)_2$ with N,N,N',N'-tetraisobutylpyridine-2,6-dithiocarboxamides (S-dbpt), N,N,N',N'-tetraisopropyl pyridine-2,6-dithiocarboxamides (S-dppt), and N,N,N',N'-tetraethylpyridine-2,6-dithiocarboxamides (S-dept) lead to the formation of $[\text{Co}(\text{S-dbpt})\text{Br}_2]$ (1), $[\text{Co}(\text{S-dppt})(\text{SCN})_2]$ (2), and $[\text{Ni}(\text{S-dept})_2] \cdot (\text{ClO}_4)_2 \cdot \text{H}_2\text{O}$ (3), respectively. The X-ray crystal structures of the three S-dapt ligands and three complexes along with spectroscopic analyzes are presented. The molecular structure investigations of the S-dapt ligands show that the thiamide planes are twisted with respect to the pyridine ring, which is more in the case of phenyl groups. The structures of the Co(II) complexes reveal that an increase in steric crowding on the amide side arms of the ligands has no substantial effect on the geometry adopted by the corresponding complexes. The Co(II) gives only 1 : 1 five-coordinate, ion-paired complexes with a distorted square pyramidal geometry. Ni(II), on the other hand, prefers an octahedral geometry with 1 : 2 metal–ligand ratio. The coordination behavior of S-dapt has been compared to the analogous oxo(O-daap) ligands. Lesser propensity of S atom to get involved in H-bonding interactions ensures an S–N–S type of tridentate coordination by S-dapt.

Keywords: Tetraalkylpyridine-2, 6-Dithiocarboxamides; Five-coordinate; X-ray crystal structure; Thermal analysis; Hydrogen bonding interactions

1. Introduction

Among various ligands derived from pyridine-2,6-dicarboxylic acid, there has been a growing interest in the development of the coordination chemistry of pyridine dicarboxamide ligands [1–13]. The carboxamide $[-\text{C}(\text{O})\text{NH}-]$ group present in the primary structure of proteins is an important ligand construction unit for coordination chemists. These ligands exhibit a range of coordination numbers, geometries, and nuclearities for transition metal and lanthanide ions. Upon deprotonation of carboxamide nitrogen atoms, these centers and the pyridyl ring nitrogen of the anion chelate to the metal ions. Recently, a whole new class of ligands having fully substituted amide nitrogens, N,N,N',N'-tetraalkyl-

*Corresponding author. Email: hundal_chem@yahoo.com

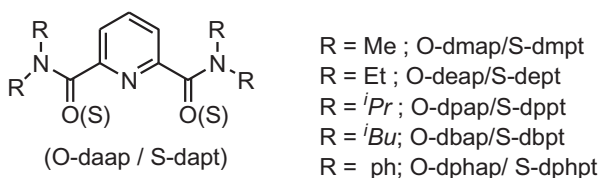
pyridine-2,6-dicarboxamides (O-daap) (scheme 1), was synthesized and characterized by us [14–19] and others [20–24]. The symmetrical tertiary amide side arms at the 2- and 6-positions of the central pyridine ring provide a variety of novel *O~N~O* and *S~N~S* tridentate receptors for binding to metal ions.

In order to investigate the effect of change in the donor set of atoms in the two side arms of the ligand on the coordination geometry adopted by the complexes, we have carried out studies on N,N,N',N'-tetraalkylpyridine-2,6-dithiocarboxamides (S-dapt) ligands [15, 25–28] (scheme 1). It is envisaged that the substitution of the donor atoms by atoms of different size and electronegativity (i.e. S in place of O) may be reflected by major changes in the coordination geometries and solid state structures adopted by the corresponding complexes. Crystal structures of Cu(II) complexes with S-dept and O-deap ligands have already shown important differences. For example, $[\text{Cu}_2\text{Cl}_2(\mu\text{-S-dept})_2][\text{Cu}_2\text{Cl}_4(\mu\text{-Cl})_2]$ is a tetranuclear Cu(II) complex formed by a cationic $[\text{Cu}_2\text{Cl}_2\{\mu\text{-S-dept}\}_2]^{2+}$ and an anionic dinuclear complex $[\text{Cu}_2\text{Cl}_4(\mu\text{-Cl})_2]^{2-}$ [25]. Also the complex $[\text{Cu}_2(\mu\text{-Cl})_2(\text{S-dept})_2][\text{CuCl}_3(\text{EtOH})_2]$, which is prepared in a similar manner but using ethanol instead of acetonitrile, consists of a cationic binuclear moiety, $[\text{Cu}_2(\mu\text{-Cl})_2(\text{S-dept})_2]^{2+}$, and two close anionic species with formula $[\text{CuCl}_3(\text{EtOH})]^-$ conforming a *pseudo*-dinuclear unit. In the cationic fragment, each copper is five-coordinate by the pyridine N atom and the two S atoms of the S-dept ligand, as well as by two chloro ligands acting in a bridging mode [25]. On the other hand, $\text{CuCl}_2(\text{O-deap})$ is a five-coordinate, trigonally distorted rectangular pyramidal complex [14]. The crystal and molecular structure of a 2 : 1 complex of CoCl_2 with S-dept has been determined. The compound is built up from $[\text{Co}(\text{S-dept})(\text{Cl})]^{+}$ and $[\text{Co}_2\text{Cl}_4(\mu\text{-Cl})_2]^{2-}$ units [28]. Hence, the substitution of S in place of O in the pyridine dicarboxamide complexes has manifested its effect on their nuclearity, coordination geometry, and solid state structures, and thus points towards yet another exciting and scarcely studied aspect of the carboxamide chemistry. In continuation of our studies on the ligation behavior of these tridentate ligands (S-dapt) with *S~N~S* donor set of atoms, in this article, we present the synthesis, molecular, and crystal structure investigations of three ligands (S-dept, S-dbpt, and S-dphpt) and three new M(II)-(S-dapt) coordination complexes (M(II) = Co(II), Ni(II); $[\text{Co}(\text{S-dbpt})\text{Br}_2]$ (1), $[\text{Co}(\text{S-dppt})(\text{SCN})_2]$ (2), and $[\text{Ni}(\text{S-dept})_2] \cdot (\text{ClO}_4)_2 \cdot \text{H}_2\text{O}$ (3).

2. Experimental setup

2.1. General

All reactions leading to the synthesis of S-dapt ligands were carried out in anhydrous solvents under dry N_2 atmosphere. Solvents and other reagents were dried using standard techniques as described earlier [29].



Scheme 1.

2.2. Preparation of ligands

- (a) *N,N,N',N'*-tetraethylpyridine-2,6-dithiocarboxamide (*S-dept*) [25, 26].
 (b) *N,N,N',N'*-tetraisopropylpyridine-2,6-dithiocarboxamide (*S-dppt*) [27].
 (c) *N,N,N',N'*-tetraisobutylpyridine-2,6-dithiocarboxamide (*S-dbpt*) [27].
 (d) *N,N,N',N'*-tetraphenylpyridine-2,6-dithiocarboxamide (*S-dphpt*): The ligand *N,N,N',N'*-tetraphenylpyridine-2,6-dithiocarboxamide (*S-dphpt*) was prepared as per the method given for *S-dept*, except that *N,N,N',N'*-tetraphenylpyridine-2,6-dicarboxamide (*O-dphap*) was used as the starting materials. The latter compound was obtained as a white solid by using a similar method as reported for the preparation of *O-deap* but using diphenylamine instead. *O-dphap*: color: white m.p., 181 °C. Anal. Calcd for $C_{31}H_{23}N_3O_2$: C, 79.30; H, 4.90; N, 8.88%. Found: C, 79.31; H, 4.90; N, 8.85%. 1H NMR ($CDCl_3$, TMS): δ 6.96 (m, 12H, ph), 7.22 (m, 8H, ph), 7.29 (d, 2H, py) 7.62 (t, 1H, py). IR (KBr pellet, cm^{-1}): μ_{CO} : 1644. *S-dphpt*: color: orange m.p., 200 °C. Anal. Calcd for $C_{31}H_{23}N_3S_2$: C, 74.25; H, 4.50; N, 8.38; S, 12.77%. Found: C, 73.68; H, 3.97; N, 7.98; S, 12.15%. 1H NMR ($CDCl_3$, TMS): δ 6.98 (m, 12H, ph), 7.23 (m, 8H, ph), 7.28 (d, 2H, py), 7.63 (t, 1H, py). IR (KBr pellet, cm^{-1}): 1587 m, 1565 m, 1461 s, 1304s, 1280 m, 1226 m, 1157 m, 1093 m, 1073 m, 1051 m, 1023 m, 803 m, 771 m, 763 m, 744 s, 722 s, 696 s, 633 m, 594 s.

2.3. Preparation of complexes

2.3.1. $[Co(S-dbpt)Br_2]$ (1). Anhydrous $CoCl_2$ (4 mM), dissolved in anhydrous ethanol (20 mL), was added to a solution of KBr (8 mM) in ethanol (20 mL). The mixture was refluxed for about 4 h. The white precipitates of KCl were removed by filtration and *S-dbpt* (4 mM), dissolved in ethanol (20 mL), was added to the solution. After refluxing for about 5 h, **1** was obtained as dark green solid on keeping at room temperature. The complex was crystallized from acetonitrile by slow evaporation at room temperature. Color: dark green m.p., 235 °C. Anal. Calcd for $C_{23}H_{39}Br_2CoN_3S_2$: C, 43.12; H, 6.14; N, 6.56; S, 10.01. Found: C, 42.92; H, 5.94; N, 6.42; S, 9.88%. Molar conductance ($\Omega^{-1} cm^2 M^{-1}$): 30 (CH_3CN) (expected ranges for 1:1 and 1:2 electrolytes in CH_3CN are 120–160 and 220–380, respectively). IR (KBr pellet, cm^{-1}): 1615 s, 1447 m, 1368 w, 1311 w, 1248 w, 1164 w, 1081 w, 820 m, 643 w, 498 w, 468 w.

2.3.2. $[Co(S-dppt)(SCN)_2]$ (2). Anhydrous $CoCl_2$ (3 mM), dissolved in anhydrous ethanol (20 mL), was added to a solution of KSCN (6 mM) in ethanol (20 mL). The mixture was refluxed for about 4 h. The white precipitate of KCl was removed by filtration and *S-dppt* (4 mM), dissolved in ethanol (20 mL), was added to the solution. After refluxing for about 4 h, **2** was obtained as green solid on keeping at room temperature. The complex was crystallized from acetonitrile by slow evaporation at room temperature. Color: green m.p., 215 °C. Anal. Calcd for $C_{21}H_{31}CoN_5S_4$: C, 46.65; H, 5.78; N, 12.95; S, 23.72. Found: C, 46.34; H, 5.66; N, 12.82; S, 23.68. Molar conductance ($\Omega^{-1} cm^2 M^{-1}$): 32 (MeCN) and 28 (DMF). IR (KBr pellet, cm^{-1}): 2055 s, 1623 m, 1582 w, 1541 m, 1486 m, 1401 m, 1305 m, 1219 w, 1178 w, 1154 m, 1056 w, 1012 w, 989 w, 821 w, 662 w, 440 w.

2.3.3. $[Ni(S-dept)_2] \cdot (ClO_4)_2 \cdot H_2O$ (3). Anhydrous $NiCl_2$ (4 mM), dissolved in anhydrous ethanol (20 mL), was added to a solution of $NaClO_4$ (8 mM) in dry ethanol (20 mL). The mixture was refluxed for about 4 h. The white precipitates of NaCl were removed by filtration and *S-dept* (4 mM), dissolved in ethanol (20 mL), was added to the solution. After refluxing for about 4 h, **3** was obtained as reddish brown solid on keeping at room

temperature. The complex was crystallized from acetonitrile by slow evaporation at room temperature. Color: reddish brown m.p., 255 °C. Anal. Calcd for $C_{30}H_{48}N_6S_4NiO_9Cl_2$: C, 40.28; H, 5.41; N, 7.68; S, 14.34. Found: C, 40.44; H, 5.48; N, 7.48; S, 14.28. Molar conductance ($\Omega^{-1} \text{ cm}^2 \text{ M}^{-1}$): 254 (CH_3CN) (expected ranges for 1 : 1 and 1 : 2 electrolytes in CH_3CN are 120–160 and 220–380, respectively). IR (KBr pellet, cm^{-1}): 1581 w, 1511 m, 1451 w, 1379 w, 1262 m, 1094 s, 1145 w, 1094 s, 915 w, 808 w, 670 w, 623 m; ν_{OH} : 3425 br; $\nu_{\text{ClO}_4^-}$: 1094 s and 623 m.

2.4. Physical methods

Elemental analyzes (C, H and N) were performed on a Perkin-Elmer model 2400 CHN analyzer. IR spectra were recorded as KBr pellets on a Perkin-Elmer RX-1 FTIR spectrophotometer. Thermal analyzes were carried out on a Shimadzu-DTG 60 analyzer. ^1H NMR spectra of ligands were recorded on a 300 MHz JEOL FT NMR spectrometer with TMS as the reference compound. UV–vis spectra were recorded on a Shimadzu Pharmaspec UV-1700 UV–vis spectrophotometer. Molar conductance values of millimolar solutions of the complexes were measured on a conductivity bridge-Digital Conductivity Meter CC 601.

2.5. X-ray crystallography

Crystallization of ligands (S-dept, S-dbpt, and S-dphpt) and complexes (**1–3**) by very slow evaporation of their saturated solutions in ethanol and acetonitrile, respectively, at room temperature yielded suitable single crystals for X-ray analysis. The data for S-dept, S-dbpt, and **1–3** were collected at 298 K on a Siemens P4 Single-crystal X-ray diffractometer using the XSCANS package. The data were collected by the θ – 2θ scan mode with a variable scan speed up to a maximum of $2\theta = 60^\circ$ using graphite-monochromated Mo- $K\alpha$ radiation ($\lambda = 0.71073 \text{ \AA}$). To monitor the stability of the crystal, three standard reflections were measured after every 97 reflections. A psi-scan absorption correction was applied.

The data for S-dphpt were collected on a Bruker AXS KAPPA APEX-II CCD diffractometer (monochromatic Mo- $K\alpha$ radiation) equipped with an Oxford cryosystem 700Plus. Unit cell refinement, data reduction, and integration were performed by SAINT V7.68A (Bruker AXS, 2009) and data scaling was performed by SADABS V2008/1 (Bruker AXS).

All the data were corrected for Lorentz and polarization effects. The structures were solved by direct methods using SIR97 [30] and refined by full-matrix least-squares refinement techniques on F^2 using SHELXL-97 [31] in the WINGX package [32] of programs. All nonhydrogen atoms were refined anisotropically. Hydrogens of uncoordinated water in **3** were located through difference Fourier calculations and were not refined. All other hydrogens were attached geometrically riding on their respective carrier atoms with U_{iso} being 1.5, 1.2, and 1.2 times the U_{iso} of their carrier methyl, methylene, and aromatic carbon atoms, respectively. The crystal data and refinement details for S-dapt are given in table 1 and that for **1–3** are provided in table 2.

3. Results and discussion

3.1. IR and UV–vis studies

Complexes **1–3** are obtained in good yield by mixing equimolar amounts of S-dapt ligands and the appropriate metal salts in anhydrous ethanol. The compounds are readily soluble in

Table 1. Crystal data and structure refinement for S-dept, S-dbpt, and S-dphpt.

	S-dept	S-dbpt	S-dphpt
Empirical formula	C ₁₅ H ₂₃ N ₃ S ₂	C ₂₃ H ₃₉ N ₃ S ₂	C ₃₁ H ₂₃ N ₃ S ₂
Formula weight	309.48	421.69	501.64
<i>T</i> [K]	296(2)	296(2)	296(2)
Space group	<i>P</i> 2 ₁ / <i>n</i>	<i>P</i> 2 ₁ / <i>c</i>	<i>P</i> 2 ₁ / <i>c</i>
<i>a</i> [Å]	6.849(5)	11.163(5)	16.0429(12)
<i>b</i> [Å]	12.140(4)	17.901(4)	8.0781(6)
<i>c</i> [Å]	20.658(3)	13.490(3)	21.3781(17)
β [°]	90.460(5)	101.670(5)	109.000(4)
Volume [Å ³]	1717.6(14)	2640.0(14)	2619.6(3)
<i>D</i> _{Calcd} (Mg/m ³)	1.197	1.061	1.272
Absorption coefficient [mm ⁻¹]	0.305	0.214	0.228
Reflections collected/unique	3488/3199	5157/4881	33,318/5282
Data/restraints/parameters	3199/0/181	4881/0/253	5282/0/325
Final <i>R</i> indices [<i>I</i> > 2 sigma(<i>I</i>)]	<i>R</i> ₁ = 0.0449 <i>wR</i> ₂ = 0.1435	<i>R</i> ₁ = 0.0990 <i>wR</i> ₂ = 0.2214	<i>R</i> ₁ = 0.0539 <i>wR</i> ₂ = 0.1645
<i>R</i> indices (all data)	<i>R</i> ₁ = 0.0793 <i>wR</i> ₂ = 0.1803	<i>R</i> ₁ = 0.2755 <i>wR</i> ₂ = 0.3158	<i>R</i> ₁ = 0.0786 <i>wR</i> ₂ = 0.1888
CCDC No.	810,473	810,472	810,474

Table 2. Crystal data and structure refinements for 1–3.

	1	2	3
Empirical formula	C ₂₃ H ₃₉ Br ₂ CoN ₃ S ₂	C ₂₁ H ₃₁ CoN ₅ S ₄	C ₃₀ H ₄₈ Cl ₂ N ₆ NiO ₉ S ₄
Formula weight	640.44	540.68	894.59
<i>T</i> [K]	296(2)	296(2)	295(2)
Space group	<i>P</i> 2 ₁ / <i>n</i>	<i>P</i> 2 ₁ / <i>c</i>	<i>P</i> -1
<i>a</i> [Å]	10.880(4)	11.612(2)	11.911(5)
<i>b</i> [Å]	18.808(5)	14.651(4)	12.288(3)
<i>c</i> [Å]	15.055(3)	16.524(3)	15.490(5)
α [°]	90	90	91.691(4)
β [°]	108.801(5)	105.130(10)	104.711(5)
γ [°]	90	90	109.442(5)
Volume [Å ³]	2916.3(14)	2713.7(10)	2051.6(12)
<i>D</i> _{Calcd} (Mg/m ³)	1.459	1.323	1.448
Absorption coefficient [mm ⁻¹]	3.487	0.958	0.862
Reflections collected/unique	5734/5437	5282/5024	8052/7637
Final <i>R</i> indices [<i>I</i> > 2 sigma(<i>I</i>)]	<i>R</i> ₁ = 0.0544 <i>wR</i> ₂ = 0.1426	<i>R</i> ₁ = 0.0390 <i>wR</i> ₂ = 0.1148	<i>R</i> ₁ = 0.0657 <i>wR</i> ₂ = 0.1594
<i>R</i> indices (all data)	<i>R</i> ₁ = 0.1037 <i>wR</i> ₂ = 0.1617	<i>R</i> ₁ = 0.0504 <i>wR</i> ₂ = 0.1233	<i>R</i> ₁ = 0.1048 <i>wR</i> ₂ = 0.1852
CCDC No.	810,475	810,476	810,477

common organic solvents such as chloroform, CH₂Cl₂, and 1,2-dichloroethane and are stable in air. The relatively high conductivity value for **3** as compared to the other complexes clearly shows the presence of ionic moieties. The expected positive shifts in position and changes in intensity of the principal IR bands of the pyridine ring are interpreted in support of the coordination of the ligands through the pyridine ring nitrogen atom in all the complexes. The presence of a band at 2055 cm⁻¹ in **2** is consistent with *N*-bonded terminal thiocyanato groups. The presence of ionic perchlorates in **3** is indicated by the characteristic band at 1094 cm⁻¹ and a weaker absorption at 623 cm⁻¹, while a broad band at 3425 cm⁻¹ is attributed to the presence of uncoordinated water.

The UV–vis spectrum of **1** was investigated in methanol at room temperature (figure S1 (see online supplemental material at <http://dx.doi.org/10.1080/00958972.2013.859679>)). In the visible region, a band is observed with a maxima around 680 nm ($14,705\text{ cm}^{-1}$; $\epsilon = 391\text{ M}^{-1}\text{ cm}^{-1}$) along with a shoulder at 600 nm ($16,666\text{ cm}^{-1}$; $\epsilon = 279\text{ M}^{-1}\text{ cm}^{-1}$). This multiple structured feature is the result of overlapping between two neighboring bands in this region and is characteristic of five-coordinated Co(II) square pyramidal complexes [33]. Similarly, for **2**, a band around 690 nm ($14,492\text{ cm}^{-1}$; $\epsilon = 350\text{ M}^{-1}\text{ cm}^{-1}$) is observed with a shoulder around 670 nm ($14,925\text{ cm}^{-1}$; $\epsilon = 330\text{ M}^{-1}\text{ cm}^{-1}$) in the visible region corresponding to the d-d transitions (Supplemental data figure S2).

Generally, three spin allowed transitions from $^3A_{2g} \rightarrow ^3T_{2g}$, $^3A_{2g} \rightarrow ^3T_{1g}(F)$, and $^3A_{2g} \rightarrow ^3T_{1g}(P)$ falling within the range 800–1400, 550–900, and 380–530 nm, respectively, are observed for Ni(II) octahedral complexes [33]. The electronic absorption spectrum of **3** recorded in acetonitrile showed (Supplemental data figure S3) two broad bands in the visible region. One broad band is found in the region 580–620 nm with λ_{max} at 600 nm ($16,616\text{ cm}^{-1}$; $\epsilon = 96\text{ M}^{-1}\text{ cm}^{-1}$) and the other one as a shoulder at 420 nm ($23,809\text{ cm}^{-1}$; $\epsilon = 380\text{ M}^{-1}\text{ cm}^{-1}$) which have been assigned to spin-allowed d-d transition bands of $^3A_{2g} \rightarrow ^3T_{1g}(F)(\nu_2)$ and $^3A_{2g} \rightarrow ^3T_{1g}(P)(\nu_3)$, respectively, by comparison with the literature. The ν_1 band has not been seen, which would probably be lying in the near infrared region beyond 1100 nm.

3.2. Thermal studies

The thermogravimetric analysis performed on **1** is shown in figure 1. The pyrolysis curve shows that the complex is thermally very stable as it starts losing weight only above 200 °C. Beyond this temperature, it loses weight very rapidly and up to 548 °C the organic ligand S-dbpt is lost from the complex (Calcd wt. loss, 65.8; obs. wt. loss, 64.7%). From 550 °C onwards till 600 °C, the complex loses the two bromide entities, as the total weight loss suffered by the present complex **1** from beginning to 600 °C corresponds to CoS being left as residue in the end (Calcd wt. loss, 24.8; obs. wt. loss, 23.5%).

The thermogravimetric analysis on **2** (figure 2) shows the presence of a solvent molecule methanol which loses around 100 °C (obs. wt. loss, 5.3%; Calcd wt. loss, 5.5%). The complex itself is stable to 250 °C whereupon the organic part is decomposed in three steps to leave a mixture of thocyanates and sulfides of cobalt(II) (obs. wt. loss, 59.8%; Calcd wt. loss, 60.2%).

Complex **3** (figure 3) loses weight in two major steps. In the first step, between 130 and 138 °C, it undergoes weight loss corresponding to the two waters present in the crystal lattice (obs. wt. loss, 2.2; Calcd wt. loss, 2.0%). The compound is thermally very stable as even the lattice water is lost only above 130 °C. This can be explained by having an insight into of the crystal structure of the complex in which hydrogen-bonded water dimers are encapsulated in a cage formed by extensive intermolecular hydrogen bonding interactions between the complex molecules and perchlorates. The anhydrous product formed after the removal of lattice water is stable to 270 °C. Beyond this temperature, in the second step, it loses weight very rapidly up to 300 °C, and finally the loss of organic ligand molecules along with the two perchlorate moieties gives NiS as the residue at the end at 400 °C (obs. wt. loss, 88.9; Calcd wt. loss, 88.2%). Thereafter, it does not suffer any weight loss up to 600 °C.

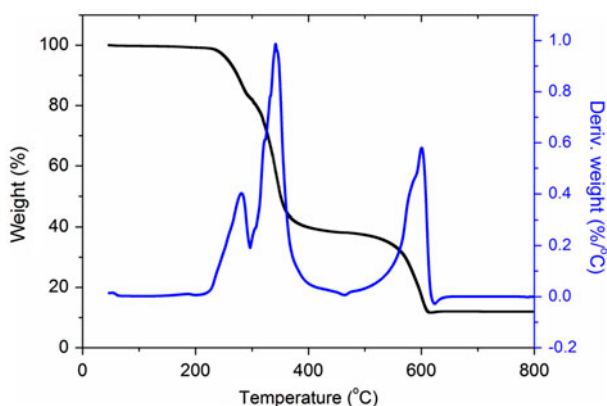


Figure 1. Thermogravimetric analysis (TGA) data of **1** as a function of temperature up to 800 °C (black line). The negative of the first derivative is also plotted as a function of temperature (blue line) (see <http://dx.doi.org/10.1080/00958972.2013.859679> for color version).

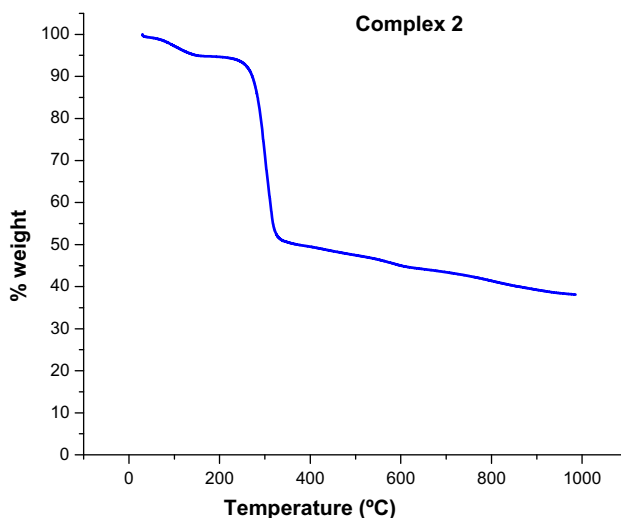


Figure 2. Thermogravimetric analysis (TGA) data of **2** as a function of temperature up to 1000 °C.

3.3. Molecular and crystal structures of *N,N,N',N'*-tetraalkylpyridine-2,6-dithiocarboxamide (*S*-dapt) ligands

3.3.1. *N,N,N',N'*-tetraethylpyridine-2,6-dithiocarboxamide (*S*-dept). A search of the Cambridge Crystal Structure Database revealed that although the crystal structures of complexes with *S*-dept and *S*-dbpt have been reported, the molecular and crystal structure investigations of the ligands have never been undertaken. To the best of our knowledge, there are no molecular and crystal structure reports regarding *S*-dphpt either in any complex or as an uncoordinated ligand.

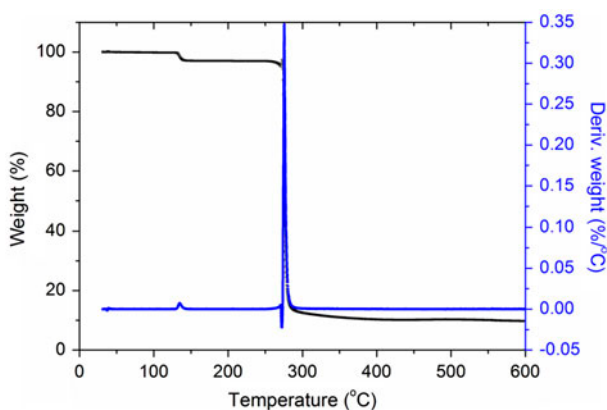


Figure 3. Thermogravimetric analysis (TGA) data of **3** as a function of temperature up to 600 °C (black line). The negative of the first derivative is also plotted as a function of temperature (blue line) (see <http://dx.doi.org/10.1080/00958972.2013.859679> for color version).

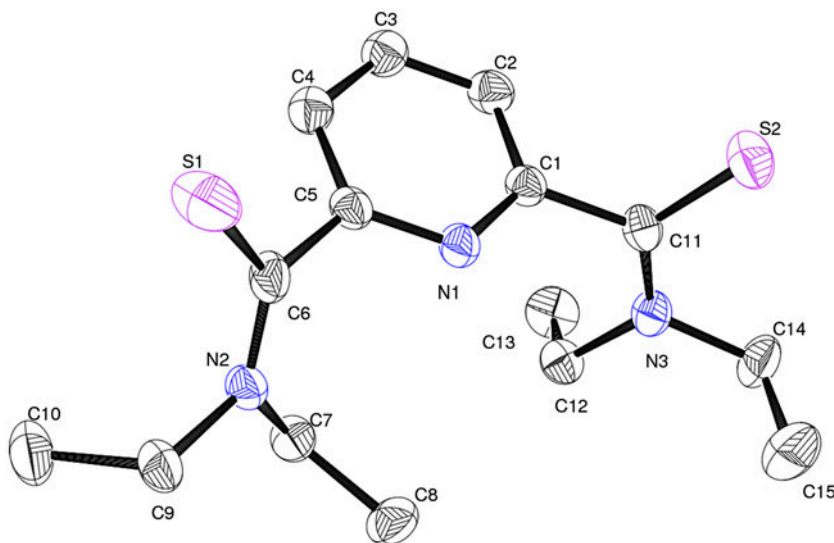


Figure 4. ORTEP diagram and labeling scheme used for S-dept. Ellipsoids are drawn at 50% probability level.

Figure 4 shows the ORTEP representation and atom numbering scheme for N,N,N',N'-tetraethylpyridine-2,6-dithiocarboxamide (S-dept). It consists of a pyridine ring with two amide side arms at 2 and 6 positions. The amide nitrogen atom of each side arm is fully substituted with two ethyl groups. The torsion angles of 75.8(3)° (C2–C1–C11–S2) and –60.5(3)° (C4–C5–C6–S1) show that the thiamide groups are much “twisted out” from the plane of the pyridine ring. This may be attributed to the steric factors due to the presence of ethyl groups on the fully substituted thiamide nitrogen atoms. For pyridine-3-thiamide [34–36], the corresponding torsion angles are –35.69 and –36.96°, respectively, indicating that in this case the thiamide moieties are relatively less twisted out from the pyridine ring

plane. Furthermore, the C=S groups are “flipped out” or are in *trans* orientation with respect to the pyridine nitrogen atom N1 as is evident from the torsion angles (N1–C5–C6–S1) 118.0(2)° and (N1–C1–C11–S2) as –103.3(3)°. Upon complexation to metal ion, these C=S groups “flip inwards” to coordinate to the metal ion and become *cis* to pyridine nitrogen atom, and thus the ligand coordinates in a tridentate fashion through the two C=S groups and pyridine nitrogen atom.

The orientations of the terminal carbon atoms on the fully substituted amide nitrogen atoms is such that the atoms C8 and C15 are above their corresponding amide planes while the atoms C10 and C13 are below, so as to minimize steric strain in the structure (Supplemental data figure S4). Important bond lengths and angles are listed in table 3. The C15–H15B⋯S2ⁱ (2.88 Å) and C12–H12B⋯S2ⁱ (2.85 Å, where *i* = *x* + 1, +*y*, +*z*) intermolecular hydrogen bonding interactions hold the ligand molecular together in the crystal lattice to form a 1-D chain running along the *a* axis. These parallel chains are in turn interlinked through C4–H4⋯S2ⁱⁱ (2.83 Å, ii = –*x* – 1/2, +*y* + 1/2, –*z* + 1/2) hydrogen bonding interactions to give rise to a 2-D corrugated sheet parallel to the *ab* plane (Supplemental data figure S5).

3.3.2. N,N,N',N'-tetraisobutylpyridine-2,6-dithiocarboxamide (S-dbpt). Figure 5 shows the ORTEP diagram and labeling scheme used in the structure analysis of N,N,N',N'-tetraisobutylpyridine-2,6-dithiocarboxamide (S-dbpt). The molecular structure of S-dbpt

Table 3. Important bond lengths [Å] and angles [°] for S-dept, S-dbpt, and S-dphpt.

<i>S-dept</i>			
S2–C11	1.653(3)	S1–C6	1.664(3)
N2–C6	1.322(4)	N2–C9	1.467(3)
N2–C7	1.477(3)	C1–N3	1.325(4)
C11–C1	1.500(4)	N3–C12	1.472(4)
N3–C14	1.479(4)	C1–N1	1.342(3)
C1–C2	1.383(4)	N1–C5	1.338(3)
N2–C6–S1	124.8(2)	C5–C6–S1	116.6(2)
N3–C11–S2	125.4(2)	C1–C11–S2	117.3(2)
C6–N2–C9	120.9(2)	C6–N2–C7	124.2(2)
C9–N2–C7	114.9(2)	N3–C11–C1	117.3(2)
C11–N3–C12	123.6(2)	C11–N3–C14	120.8(2)
<i>S-dbpt</i>			
C6–S1	1.660(7)	C15–S2	1.654(8)
C1–N1	1.357(9)	C5–N1	1.332(9)
C6–N2	1.339(9)	C7–N2	1.470(9)
C11–N2	1.461(3)	C15–N3	1.327(9)
N3–C15–S2	125.7(7)	C1–C15–S2	115.4(6)
N1–C1–C2	121.9(8)	N1–C1–C15	115.3(7)
N1–C5–C4	122.5(8)	N1–C5–C6	116.3(7)
C4–C5–C6	121.2(8)	N2–C6–C5	117.8(6)
N2–C6–S1	125.6(6)	C5–C6–S1	116.6(6)
C9–C8–C7	107.4(8)	N2–C11–C12	113.7(7)
<i>S-dphpt</i>			
C1–N1	1.333(3)	C1–C2	1.380(3)
C5–N1	1.334(3)	C5–C4	1.387(3)
C5–C6	1.505(3)	C6–N2	1.343(3)
C6–S1	1.646(2)	C7–C12	1.375(4)
C7–C8	1.388(3)	C7–N2	1.447(3)
N1–C1–C2	123.6(2)	N1–C1–C19	115.81(19)
C2–C1–C19	120.4(2)	N1–C5–C4	123.5(2)
N1–C5–C6	114.77(19)	C4–C5–C6	121.7(2)
N2–C6–C5	116.1(2)	N2–C6–S1	125.88(17)

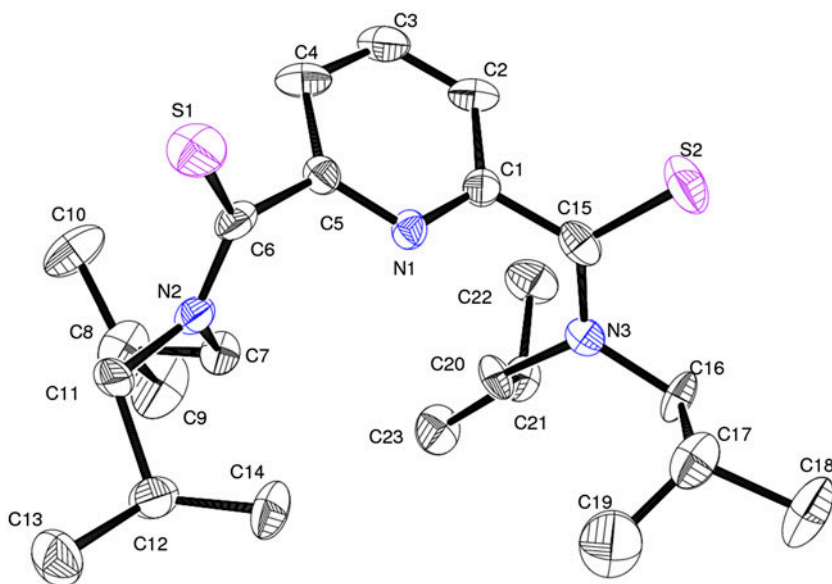


Figure 5. ORTEP diagram and labeling scheme used in the structure analysis of S-dbpt. Ellipsoids are drawn at 50% probability level.

is essentially the same as for S-dept, only difference being the nature of alkyl groups on the thiamide nitrogen atoms. In S-dbpt, there are bulky *isobutyl* groups on thiamide nitrogen atoms N1 and N2. Owing to steric factors, the thiamide moieties are twisted away from the pyridine ring plane as indicated by torsion angles of $61.3(3)^\circ$ (C4–C5–C6–S1) and $-65.2(4)^\circ$ (C2–C2–C15–S2) and are *trans* to the pyridine N1, because of the torsion angles $112.9(6)^\circ$ (N1–C5–C6–S1) and $-115.2(6)^\circ$ (N1–C1–C15–S2). The *isobutyl* groups on the thiamide nitrogens on the side arms of the pyridine ring are oriented in such a way so as to minimize the steric strain in the structure. C8, C9, C10, C21, C22, and C23 are oriented above their respective thiamide planes while C12, C13, C14, C17, C18, and C19 lie below (Supplemental data figure S6). Important bond lengths and angles are listed in table 3. The $C8-H8 \cdots S2^i$ (2.85 Å, $i=x-1, +y, +z$) and $C7-H7A \cdots S1^{ii}$ (2.96 Å, $ii=x, -y+1/2, +z+1/2$) intermolecular hydrogen bonding interactions lead to the formation of a 2-D sheet structure parallel to the *ac* plane (Supplemental data figure S7).

3.3.3. N,N,N',N'-tetraphenylpyridine-2,6-dithiocarboxamide (S-dphpt). The molecular structure of N,N,N',N'-tetraphenylpyridine-2,6-dithiocarboxamide (S-dphpt) is similar to S-dept and S-dbpt. Figure 6 shows the ORTEP diagram and the numbering scheme used in the structure analysis of S-dphpt. In this case, two phenyl rings are attached to each of the two nitrogens of the thioamide side arms. The usual twisting of the amide moieties with respect to the pyridine ring plane to accommodate phenyl rings is more pronounced in this case as indicated by the torsion angles being C4–C5–C6–S1 $-106.9(1)^\circ$ and C2–C1–C19–S2 $103.2(1)^\circ$. The orientation of the two twisted amide planes is such that the C=S moieties are almost *trans* to each other at the same time they are now in a *gauche* conformation *viz-a-viz* the pyridine nitrogen as is evident from the torsion angles (N1–C1–C19–S2) $-72.5(3)^\circ$ and (N1–C5–C6–S1) $-71.1(2)^\circ$.

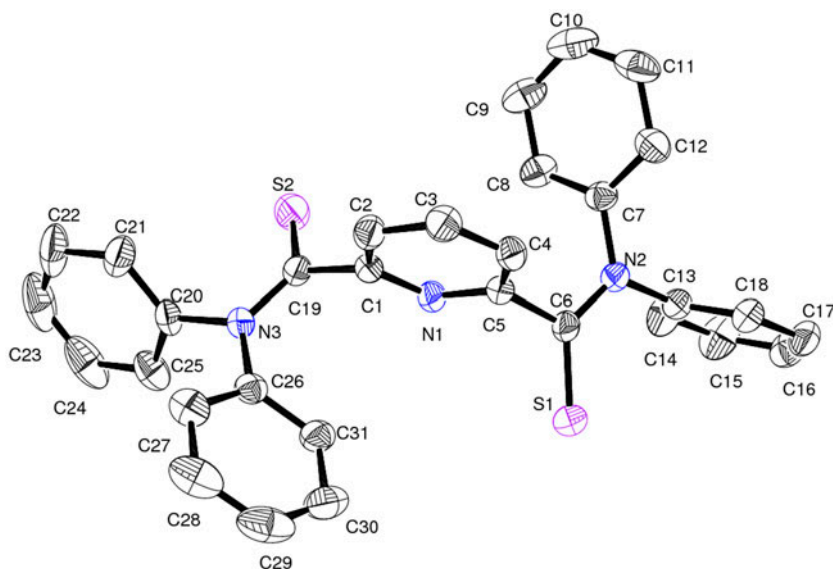


Figure 6. ORTEP diagram and atom numbering scheme used for S-dphpt. Ellipsoids are drawn at 50% probability level.

To minimize the strain in the structure, the two phenyl rings attached to the thioamide nitrogen atom N2 orient themselves in such a way that the dihedral angle between their respective planes is $68.86(3)^\circ$ (plane 1 = C7–C8–C9–C10–C11–C12 and plane 2 = C13–C14–C15–C16–C17–C18). Similarly, the dihedral angle between the planes of the two phenyl groups attached to the thioamide nitrogen atom N1 is $87.10(2)^\circ$ (plane 1 = C20–C21–C22–C23–C24–C25 and plane 2 = C26–C27–C28–C29–C30–C31) (figure 7). Important bond lengths and angles are listed in table 3. In the crystal lattice, the molecules are held together through $C4-H4 \cdots S1^i$ (2.94 Å, $i = -x + 1, -y + 1, -z + 2$) and $C9-H9 \cdots S2^{ii}$ (2.92 Å, $ii = -x, -y + 1, -z + 2$) intermolecular hydrogen bonding interactions to form a 1-D chain running parallel to the a axis. These parallel chains are in turn held together by C–H $\cdots\pi$ interactions to form a 2-D sheet structure parallel to the ab plane (Supplemental data figure S8).

3.4. Molecular and crystal structures of $M(II)$ - N,N,N',N' -tetraalkylpyridine-2,6-dithiocarboxamide complexes, $M(II) = Co(II), Ni(II)$

3.4.1. $[Co(S\text{-dbpt})Br_2]$ (1). The ORTEP diagram and the atom numbering scheme for **1** is shown in figure 8. The Co(II) ion in **1** has a five-coordinate stereochemistry with CoNS₂Br₂ chromophore. S-dbpt coordinates to the metal center in a tridentate fashion using the pyridine nitrogen and the two thioamide sulfur atoms, while the remaining two positions are occupied by two bromide groups. Important bond lengths and angles are listed in table 4. The conformation of S-dbpt around the thioamide moieties reverses itself in the complex. In **1**, both the C=S groups are “flipped in” and are in *cis* conformation to the pyridine nitrogen N1 as indicated by torsion angles (N1–C1–C15–S2) $-48.4(6)^\circ$ and (N1–C5–C6–S1) $41.9(6)^\circ$, which enables them to coordinate to the metal ion in tridentate fashion. Furthermore, to maximize the electron donation through coordination, both these thioamide moieties are

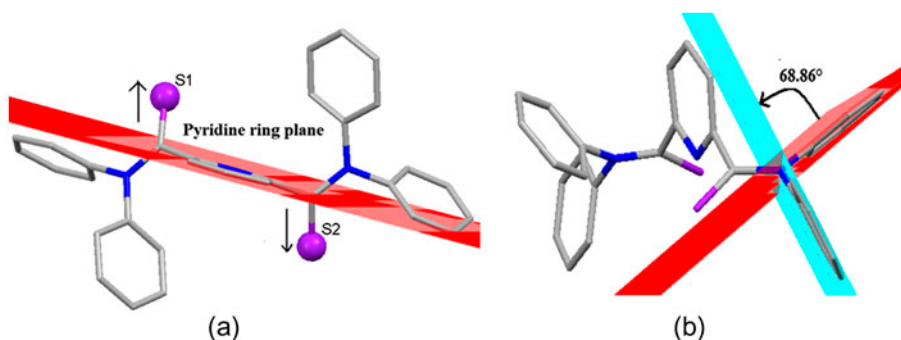


Figure 7. (a) The *trans* orientation of the two C=S groups with respect to plane of the pyridine ring and (b) the dihedral angle between planes of the two phenyl rings attached to thioamide nitrogen in S-dphpt.

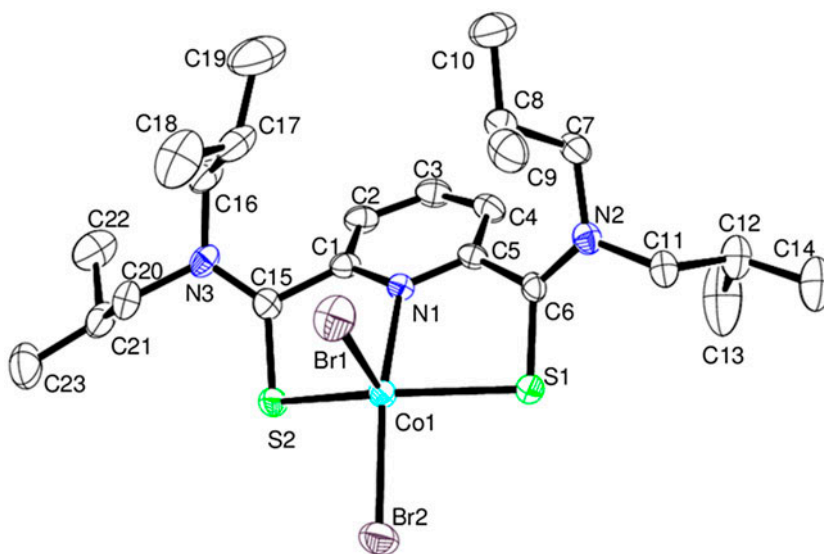


Figure 8. ORTEP diagram and atom numbering scheme for **1**. Ellipsoids are drawn at 30% probability level.

bending away from the pyridine ring plane with torsion angles (C2–C1–C15–S2) $124.8(5)^\circ$ and (C4–C5–C6–S1) $-130.7(5)^\circ$.

It is generally observed that most of the five-coordinate complexes have neither an ideal trigonal bipyramidal (*tbp*) nor square pyramidal (*sp*) environment, but their geometry falls between *sp* and *tbp* depending upon a parameter τ suggested by Addison and co-workers [37]. The parameter τ is determined by the relation $\tau = (\beta - \alpha)/60$ (where α and β are the largest basal angles with $\beta > \alpha$) and its value may vary from 0, representing ideal *sp* (square pyramidal) geometry to 1, denoting ideal *tbp* (trigonal bipyramidal) geometry. The geometry of **1** may be considered as distorted square pyramidal, τ value being 0.37 [$\beta = \text{N}(1)\text{--Co}(1)\text{--Br}(2)$, $159.73(2)^\circ$ and $\alpha = \text{S}(2)\text{--Co}(1)\text{--S}(1)$, $137.34(3)^\circ$].

In **1**, the apical position in the square pyramid is occupied by the bromine atom Br1 while sulfur atoms S1, S2, pyridine N1 and Br2 form the base of the pyramid. A mean

Table 4. Important bond lengths [Å] and angles [°] for **1** and **2**.

1			
N1–Co1	2.140(4)	S(1)–Co(1)	2.4454(17)
S2–Co1	2.4754(17)	Co(1)–Br(1)	2.4115(13)
Co1–Br2	2.4286(13)		
N1–Co1–Br1	92.88(13)	N(1)–Co(1)–Br(2)	159.73(13)
Br1–Co1–Br2	107.38(5)	N(1)–Co(1)–S(1)	79.27(13)
Br1–Co1–S1	108.93(5)	Br(2)–Co(1)–S(1)	93.39(6)
N1–Co1–S2	79.66(12)	Br(1)–Co(1)–S(2)	108.78(6)
Br2–Co1–S2	93.79(5)	S(1)–Co(1)–S(2)	137.34(6)
C6–S1–Co1	94.5(2)	C(15)–S(2)–Co(1)	92.07(19)
2			
C1–N1	1.341(3)	N1–Co	2.152(2)
N4–Co	1.996(3)	N5–Co	2.003(2)
S1–Co	2.4244(9)	S2–Co	2.3561(9)
N4–Co–N1	94.37(9)	N5–Co–N1	161.30(9)
N4–Co–S2	120.50(8)	N5–Co–S2	89.99(8)
N1–Co–S2	79.83(6)	N4–Co–S1	101.05(8)
N5–Co–S1	95.73(8)	N1–Co–S1	81.02(6)
S2–Co–S1	135.16(3)	C20–N4–Co	168.4(3)
C21–N5–Co	164.7(2)	C6–S1–Co	90.26(9)
C13–S2–Co	99.44(9)	N4–Co–N5	104.32(10)

plane can be passed through S1, S2, N1, and Br2 with -0.065 , -0.264 , 0.6164 , and 0.013 Å being deviations for these atoms from this plane, respectively. The Co(II) ion is 0.73 Å above the mean plane defined by these four atoms. The orientation of the terminal carbon atoms on the thioamide nitrogen atoms N2 and N3 is such that C13, C14, C22, and C23 are above their respective thioamide planes while C9, C10, C18, and C19 lie below. This orientation minimizes the steric strain in the structure due to bulky *isobutyl* groups on thioamide nitrogen atoms. The increase in steric bulk on the amide side arms of the ligands has no substantial effect on the geometry adopted by the corresponding complexes formed as indicated by $[\text{CoBr}_2(\text{S-dept})_2]$ [26] and the present complex $[\text{CoBr}_2(\text{S-dbpt})_2]$, both having distorted square pyramidal geometry with similar coordination environment.

The $\text{C3–H3}\cdots\text{S1}^{\text{i}}$ (2.90 Å), $\text{C4–H4}\cdots\text{Br2}^{\text{i}}$ (2.93 Å), $\text{C3–H3}\cdots\text{Br1}^{\text{i}}$ (3.12 Å, where $\text{i} = x + 1/2, -y = 1/2, +z + 1/2$), and $\text{C9–H9B}\cdots\text{Br2}^{\text{ii}}$ (3.05 Å, where $\text{ii} = -x - 1/2, +y + 1/2, -z + 1/2 + 1$) intermolecular hydrogen bonding interactions between complex molecules lead to the formation of a 2-D sheet parallel to the *ac* plane in the crystal lattice (figure 9).

3.4.2. $[\text{Co}(\text{S-dppt})(\text{SCN})_2]$ (2**).** The molecular structure of **2** is very similar to that of **1** except that there are two SCN groups in place of two bromide groups and the coordinating ligand (S-dppt) has *isopropyl* groups on the nitrogen atoms of thioamide side arms. Figure 10 shows ORTEP diagram and the numbering scheme used for **2**. The cobalt ion in the complex is five-coordinate with the S-dppt ligand molecule coordinating in a tridentate fashion, while the other two vacancies are filled by the two thiocyanate ($-\text{NCS}$) groups. The Co–S1, Co–S2, Co–N1, and Co–N(SCN) distance values are in agreement with the values reported earlier in a similar complex [26]. Important bond parameters are listed in table 4.

The conformation of S-dppt changes in a similar way in **2** as of S-dbpt in **1**. The torsion angles observed are (N1–C5–C6–S1) $-51.5(3)^\circ$, (N1–C1–C13–S2) 36.0° , (C2–C1–C13–S2) $-133.0(3)^\circ$, and (C4–C5–C6–S1) $118.7(3)^\circ$, indicating the degree to which both the coordinating C=S moieties are bending with respect to the pyridine ring plane so as to

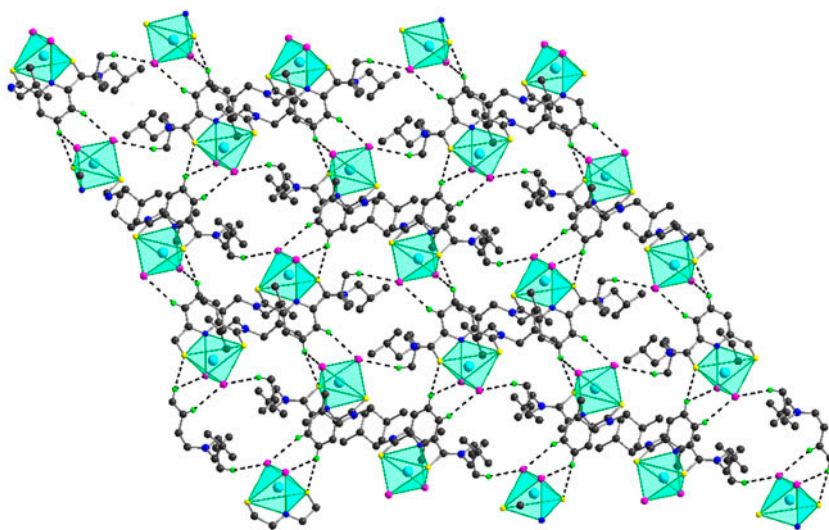


Figure 9. The 2-D sheet formed through intermolecular hydrogen bonding among complex molecules in **1**. The polyhedron (square pyramid) around each metal center is also shown.

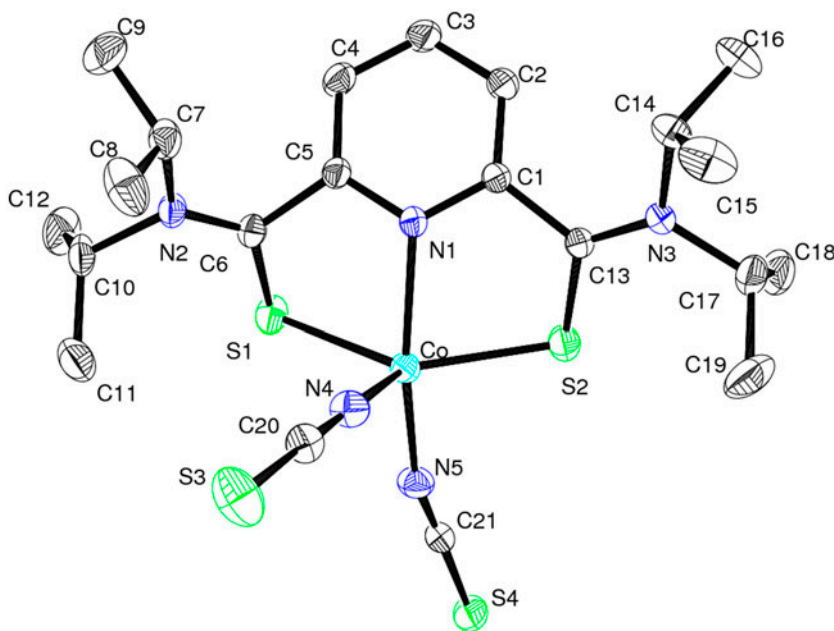


Figure 10. ORTEP diagram and atom numbering scheme for **2**. Ellipsoids are drawn at 30% probability level.

maximize electron donation by coordination to the metal ion. The geometry around the cobalt ion is distorted square pyramidal with τ value being 0.43° . The *isothiocyanate* nitrogen atom N4 occupies the apical position and sulfur atoms S1 and S2, pyridine N1 and

thiocyanate N5 form the base of the pyramid. The mean plane through N1, N5, S1, S2 indicates that these atoms are 0.39, 0.52, -0.05 , -0.08 Å, respectively, above and below the mean plane. The Co(II) ion is 0.74 Å above the mean plane defined by these four atoms. Such deviations are energetically favorable and this phenomenon is observed in most square pyramidal complexes. This has a considerable significance, since the four basal atoms effectively restrict the approach of a ligand to the sixth coordination site.

An interesting aspect of the Co–NCS linkage in **2** is the bent observed with Co–N4–C20 and Co–N5–C21 angles of $168.3(2)^\circ$ and $164.7(2)^\circ$ in the present complex as well as in another similarly coordinated complex [26]. This linkage may be either linear or angular, with examples of M–N–C angles falling in the range 141 – 174° [38, 39]. The nonlinearity of this type has been attributed to steric factors [40, 41]. The bend is more pronounced in the present complex [Co(SCN)₂(S-dbpt)] as compared in [Co(SCN)₂(S-dept)]. It also suggests electron density localization on the donor nitrogen atom such that a canonical form **I** contributes to the structure [26, 38, 42].

3.4.3. [Ni(S-dept)₂](ClO₄)₂·H₂O (3**).** Figure 11 shows the molecular structure and labeling scheme used in the structural analysis of **3**. The complex consists of discrete [Ni(S-dept)₂]²⁺ cations and perchlorate anions along with noncoordinating water molecules and has the molecular composition of [Ni(S-dept)₂](ClO₄)₂·H₂O. The nickel atom Ni1 in the complex is six-coordinate where both the ligands (S-dept) coordinate to the Ni(II) in a tridentate fashion using the pyridine nitrogen atom and both the thiocarboxamide sulfur atoms, thus bringing the metal–ligand coordinating ratio to 1 : 2. The coordinating atoms

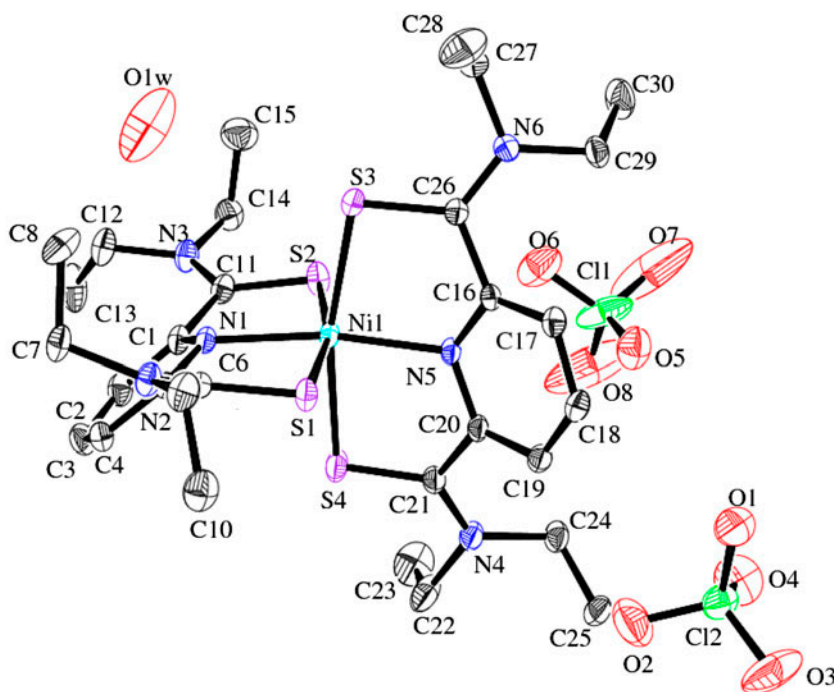


Figure 11. ORTEP diagram and atom numbering scheme for **3**. Ellipsoids are drawn at 30% probability level.

N1, S1, and S2 from one ligand molecule and N2, S3, and S4 atoms from the other coordinating ligand molecule completes the distorted octahedral geometry around Ni1. A mean plane can be passed through N1, N5, S3, and S4 forming the basal plane around the metal ion with -0.12 \AA , -0.15 \AA , $+0.017 \text{ \AA}$, and $+0.029 \text{ \AA}$ being the deviation of these atoms from this plane, respectively. The nickel atom is displaced $+0.01 \text{ \AA}$ from this plane. The distortion exhibited by the complex may be attributed to the steric hindrance caused by the ethyl groups of the thioamide moiety. S1 and S2 occupy *trans* positions in the octahedra. The important bond lengths and angles are listed in table 5. In one ligand molecule, a plane can be passed through C21, C26, N5, S3, and S4 with -0.02 \AA , $+0.09 \text{ \AA}$, -0.05 \AA , -0.005 \AA , and $+0.01 \text{ \AA}$ being deviations for these atoms from this plane, respectively. Similarly, for the other coordinating ligand molecule, C6, C11, N1, S1, and S2 define a mean plane from which these atoms are deviated by $+0.2 \text{ \AA}$, -0.12 \AA , -0.06 \AA , -0.01 \AA , and $+0.01 \text{ \AA}$. The torsion angles $91.9(2)^\circ$ (S1–Ni1–S3–C26), $-87.3(2)^\circ$ (S1–Ni1–S4–C21), $94.4(2)^\circ$ (S3–Ni1–S1–C6), and $107.3(2)^\circ$ (S3–Ni1–S2–C11) suggest that these two planes containing the coordinating atoms are approximately at right angle to each other so as to lower the steric strain and facilitate the coordination of both the ligands in the tridentate fashion to the metal ion. Furthermore, in case of each ligand molecule, the pyridine ring is bending out of the plane of the corresponding coordinating atoms to minimize the steric strain and maximize the stability of structure. This is indicated by the torsion angles values $33.3(2)^\circ$ (N1–C1–C11–S2), $-43.6(2)^\circ$ (N1–C5–C6–S1), $36.4(3)^\circ$ (N5–C16–C26–S3), and -35.0° (N5–C20–C21–S4) with respect to C1–C11, C5–C6, C16–C26, and C20–C21 bonds, respectively. Important bond lengths and angles are listed in table 5.

A comparison can be made with another transition metal complex, $[\text{Co}(\text{O-deap})_2(\text{H}_2\text{O})_2](\text{ClO}_4)_2 \cdot \text{H}_2\text{O}$ [16], involving a similar tridentate ligand O-deap coordinating to the metal center in 1 : 2 metal–ligand ratio. But in that case, one ligand molecule acts in a tridentate fashion (using the pyridine nitrogen and both the carbonyl oxygen atoms), while the other coordinates in bidentate mode using pyridine nitrogen atom and one of the carbonyl oxygens. This is due to the fact that the oxygen atom of the uncoordinated carbonyl group

Table 5. Important bond lengths [\AA] and angles [$^\circ$] for **3**.

N1–Ni1	2.064(4)	N5–Ni1	2.048(4)
S1–Ni1	2.440(2)	S2–Ni1	2.384(2)
S3–Ni1	2.398(2)	S4–Ni1	2.413(2)
O1–C2	1.425(5)	O2–C12	1.390(6)
O3–C12	1.392(5)	O4–C12	1.413(6)
O5–C11	1.372(6)	O6–C11	1.406(6)
O7–C11	1.291(11)	O8–C11	1.315(10)
S1–Ni1	2.440(2)	S2–Ni1	2.384(2)
S3–Ni1	2.398(2)	S4–Ni1	2.413(2)
N5–Ni1–N1	168.99(16)	N5–Ni1–S2	105.42(12)
N1–Ni1–S2	83.09(12)	N5–Ni1–S3	84.17(12)
N1–Ni1–S3	102.93(11)	S2–Ni1–S3	91.02(6)
N5–Ni1–S4	83.53(12)	N1–Ni1–S4	89.44(11)
S2–Ni1–S4	90.94(7)	S3–Ni1–S4	167.63(5)
N5–Ni1–S1	87.91(12)	N1–Ni1–S1	83.78(12)
S2–Ni1–S1	166.65(5)	S3–Ni1–S1	89.59(6)
S4–Ni1–S1	91.31(6)	O7–C11–O8	101.4(12)
O7–C11–O5	116.3(9)	O4–C12–O1	108.1(4)
O8–C11–O5	107.0(5)	O7–C11–O6	107.2(5)
O8–C11–O6	112.8(8)	O5–C11–O6	111.8(4)
O2–C12–O3	111.2(5)	O2–C12–O4	106.5(4)
O3–C12–O4	112.2(5)	O2–C12–O1	109.3(4)

Table 6. Important H-bonds and geometry for **3**.

D–H···A	D···A [Å]	H···A [Å]	D–H···A [°]
O2···H19 ⁱ	3.353(10)	2.66	132
O1···H18 ⁱ	3.383(9)	2.49	160
O5···H7B ⁱⁱ	3.530(9)	2.68	146
O7···H12B ⁱⁱ	3.11(2)	2.28	142
O1···H7A ⁱⁱ	3.58(1)	2.68	155
O1···H17 ⁱⁱⁱ	3.201(7)	2.44	139
O3···H28B ⁱⁱⁱ	3.48(1)	2.57	158
O3···H29B ⁱⁱⁱ	3.448(9)	2.56	152
O6···H27B ^{iv}	3.353(8)	2.56	139

i = x, y, z; ii = x + 1, y, z; iii = -x, -y, -z + 1; iv = -x, -y, -z.

strongly hydrogen bonded to the lattice water molecule. In the present case of [Ni(S-dept)₂](ClO₄)₂·H₂O, the sulfur atoms being larger in size and lower in electronegativity value as compared to oxygen atom are unable to get involved in any such strong hydrogen bonding interactions, and thus both the ligand molecules coordinate in tridentate fashion with the Ni(II) center.

The complex undergoes extensive intermolecular hydrogen bonding owing to the presence of ionic perchlorates and water molecules in crystal lattice. O1, O2, O3, O5, O6,

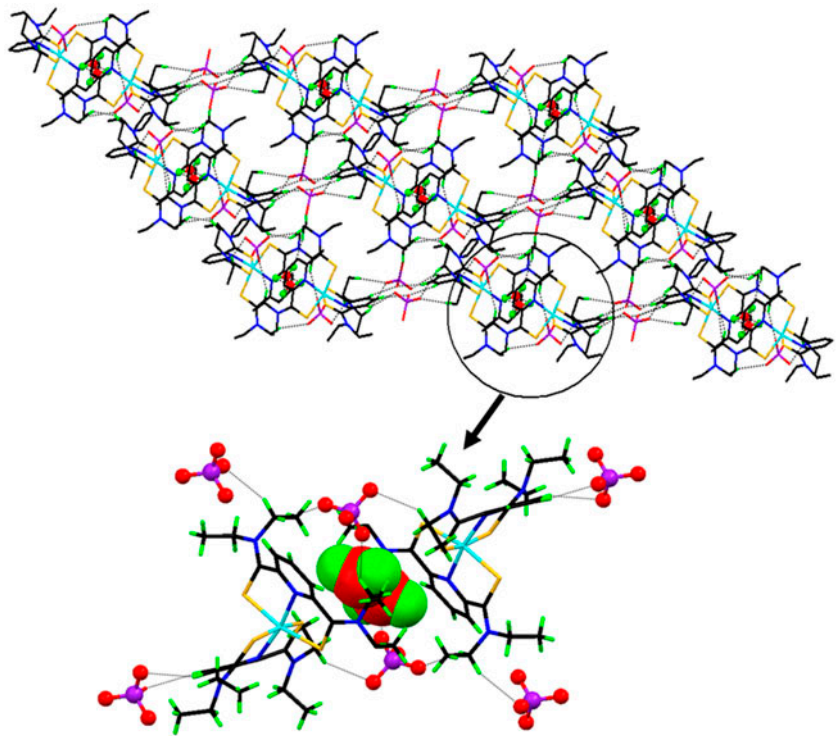


Figure 12. The extensive hydrogen bonding network involving ionic perchlorates and waters present in the crystal lattice of **3**. Two waters are shown to be encapsulated by a cage formed by the hydrogen bonding between complex molecules and perchlorates (carbon, black; hydrogen, green; nitrogen, blue; sulfur, yellow; nickel, cyan; chlorine, purple; and oxygen, red) (see <http://dx.doi.org/10.1080/00958972.2013.859679> for color version).

and O7 are involved in hydrogen bonding interactions summarized in table 6. A 2-D sheet structure is formed owing to these hydrogen bonding interactions involving perchlorates (figure 12). A close look at this type of network shows that a water dimer is trapped in a capsule made by hydrogen bonding involving two complex molecules and two perchlorates (figure 11).

4. Conclusion

In the present work, six new crystal structures are reported for three N,N,N',N'-tetraalkylpyridine-2,6-dithiocarboxamide (S-dapt) ligands and three of their complexes [Co(S-dbpt)Br₂] (**1**), [Co(S-dppt)(SCN)₂] (**2**), and [Ni(S-dept)₂](ClO₄)₂·H₂O (**3**). The molecular structure investigations of the S-dapt ligands reveal that the thiamide planes are twisted with respect to the pyridine ring plane to accommodate the alkyl/phenyl groups attached to the thiamide nitrogen. The extent of twisting depends upon the steric bulk of the alkyl/phenyl groups. These structure investigations of M(II)-(S-dapt) complexes provide ample evidence that cobalt has a greater tendency than nickel to give monomeric five-coordinate complexes rather than octahedral complexes. Furthermore, the increase in steric bulk on the amide side arms of the ligands has no substantial effect on the geometry adopted by the corresponding complexes formed as indicated by: (a) [CoBr₂(S-dept)₂] [26] and the present complex **1** [CoBr₂(S-dbpt)₂] and also (b) [Co(S-dept)(SCN)₂] [26] and the present complex **2** [Co(S-dppt)(SCN)₂]. In both the cases (a) and (b), each of the complexes has a distorted square pyramidal geometry with similar coordination environment, although having different alkyl groups on the thiamide nitrogen. The change in the donors, S in S-dapt in place of O in O-daap, ensures tridentate coordination of S-dapt as larger, and less electronegative sulfur is less likely to involve strong H-bonding interactions (with solvent or counterions) and thus is free to coordinate to the metal ion. The crystal structure investigations show the formation of 2-D sheets through C–S···H (in the case of S-dapt ligands), C–H···Br interactions (in **1**), and C–H···O (perchlorate) H-bonding interactions (in **3**).

Supplementary material

Crystallographic data for structural analysis have been deposited with the Cambridge Crystallographic Data Center (CCDC Nos. given in tables 1 and 2). Copy of this information may be obtained free of charge from The Director, CCDC, 12 Union Road, Cambridge CB2 1EZ, UK (Fax: C44 1223 336033; Email: deposit@ccdc.cam.ac.uk or <http://www.ccdc.cam.ac.uk>).

Acknowledgements

APSP and LKR thank UGC-SAP for research fellowship. PK thanks CSIR, New Delhi for financial support.

References

- [1] J.M. Rowland, M.L. Thornton, M.M. Olmstead, P.K. Mascharak. *Inorg. Chem.*, **40**, 1069 (2001).
- [2] D.S. Marlin, P.K. Mascharak. *Chem. Soc. Rev.*, **29**, 69 (2000).
- [3] (a) D.S. Marlin, M.M. Olmstead, P.K. Mascharak. *Inorg. Chim. Acta*, **297**, 106 (2000); (b) D.S. Marlin, M.M. Olmstead, P.K. Mascharak. *Inorg. Chem.*, **38**, 3258 (1999).

- [4] F.A. Chavez, J.M. Rowland, M.M. Olmstead, P.K. Mascharak. *J. Am. Chem. Soc.*, **120**, 9015 (1998).
- [5] A.K. Patra, M. Ray, R. Mukherjee. *J. Chem. Soc., Dalton Trans.*, 2461 (1999).
- [6] (a) A.K. Patra, R. Mukherjee. *Inorg. Chem.*, **38**, 1388 (1999); (b) M. Ray, D. Ghosh, Z. Shirin, R. Mukherjee. *Inorg. Chem.*, **36**, 3568 (1997).
- [7] A.K. Patra, M. Ray, R. Mukherjee. *Inorg. Chem.*, **39**, 652 (2000).
- [8] F.A. Chavez, M.M. Olmstead, P.K. Mascharak. *Inorg. Chem.*, **35**, 1410 (1996).
- [9] F.A. Chavez, C.Y. Nguyen, M.M. Olmstead, P.K. Mascharak. *Inorg. Chem.*, **35**, 6282 (1996).
- [10] S.M. Redmose, C.E.F. Rickard, S.J. Webb, L.J. Wright. *Inorg. Chem.*, **36**, 4743 (1997).
- [11] K. Hiratani, K. Taguchi. *Bull. Chem. Soc. Jpn.*, **63**, 3331 (1990).
- [12] F.A. Chavez, M.M. Olmstead, P.K. Mascharak. *Inorg. Chem.*, **36**, 6323 (1997).
- [13] A.K. Singh, V. Balamurugan, R. Mukherjee. *Inorg. Chem.*, **42**, 6497 (2003).
- [14] R. Kapoor, A. Kumar, J. Nistandra, P. Venugopalan. *Transition Met. Chem.*, **25**, 465 (2000).
- [15] R. Kapoor, A. Kataria, A. Pathak, P. Kapoor, P. Venugopalan, G. Hundal. *Polyhedron*, **24**, 1221 (2005).
- [16] R. Kapoor, A. Pathak, P. Kapoor, P. Venugopalan. *Polyhedron*, **25**, 31 (2006).
- [17] P. Kapoor, A.P.S. Pannu, M. Sharma, G. Hundal, M.S. Hundal, R. Kapoor. *J. Coord. Chem.*, **63**, 3635 (2010).
- [18] P. Kapoor, A.P.S. Pannu, M. Sharma, G. Hundal, M.S. Hundal, R. Kapoor. *J. Coord. Chem.*, **64**, 256 (2011).
- [19] P. Kapoor, A.P.S. Pannu, M. Sharma, M.S. Hundal, R. Kapoor, M. Corbella, N. Aliaga-Alcalde. *J. Mol. Struct.*, **981**, 40 (2010).
- [20] J. Garcia-Lozano, L. Soto, J.V. Folgado, E. Escrivia. *Polyhedron*, **15**, 4003 (1996).
- [21] J.G.H. du Preez, B.J.A.M. van Brecht. *Inorg. Chim. Acta*, **162**, 49 (1989).
- [22] J. Garcia-Lozano, M.A. Martinez-Lorente, E. Escrivia, R. Ballesteros. *Synth. React. Inorg. Met.-Org. Chem.*, **24**, 365 (1994).
- [23] R. Jagannathan, S. Soundarajan. *Indian J. Chem.*, **18A**, 319 (1979).
- [24] T.L. Borgne, J. Benech, S. Floquet, G. Beernardinelli, C. Aliprandini, P. Bettens, C. Piguet. *J. Chem. Soc., Dalton Trans.*, 3856 (2003).
- [25] P. Kapoor, A. Kataria, P. Venugopalan, R. Kapoor, M. Corbella, M. Rodriguez, M. Romero, A. Llobet. *Inorg. Chem.*, **43**, 6699 (2004).
- [26] R. Kapoor, A. Kataria, P. Venugopalan, P. Kapoor, G. Hundal, M. Corbella. *Eur. J. Inorg. Chem.*, **3884**, (2005).
- [27] R. Kapoor, A. Kataria, P. Kapoor, A.P.S. Pannu, M.S. Hundal, M. Corbella. *Polyhedron*, **26**, 5131 (2007).
- [28] R. Kapoor, A. Kataria, P. Kapoor, P. Venugopalan. *Transition Met. Chem.*, **29**, 425 (2004).
- [29] W.L.F. Armarego, D.D. Perrin. *Purification of Laboratory Chemicals*, 4th Edn, Butterworth-Heinemann, Oxford (1996).
- [30] A. Altomare, M.C. Burla, M. Camalli, G.L. Cascarano, C. Giacovazzo, A. Guagliardi, A.G.G. Moliterni, G. Polidori, R. Spagna. *J. Appl. Crystallogr.*, **32**, 115 (1999).
- [31] G.M. Sheldrick. *SHELXS-97, Program for the Solution of Crystal Structures*, University of Göttingen, Germany (1997).
- [32] L.J. Farrugia. *J. Appl. Crystallogr.*, **32**, 837 (1999).
- [33] A.B.P. Lever. *Inorganic Electronic Spectroscopy*, 2nd Edn, Elsevier, Amsterdam (1984).
- [34] V.R. Pedireddi, A. Ranganathan, S. Chatterjee. *Tetrahedron Lett.*, **39**, 9831 (1998).
- [35] M.S. Fonari, E.V. Ganin, S.-W. Tang, W.-J. Wang, Y.A. Simonov. *J. Mol. Struct.*, **89**, 826 (2007).
- [36] G.R. Form, E.S. Raper, T.C. Downie. *Acta Crystallogr., Sect. B: Struct. Crystallogr. Cryst. Chem.*, **29**, 776 (1973).
- [37] A.W. Addison, T.N. Rao, J. Reedijk, J. van Rijn, G.C. Verschoor. *J. Chem. Soc., Dalton Trans.*, 1349 (1984).
- [38] S.E. Livingstone. *Q. Rev. Chem. Soc.*, **19**, 386 (1965).
- [39] L.P. Battaglia, A. Bonamartini Corradi, A. Mangia. *Inorg. Chim. Acta*, **39**, 211 (1980).
- [40] D.V. Naik, W.R. Scheidt. *Inorg. Chem.*, **12**, 272 (1973).
- [41] M.G.B. Drew, A.H. Bin Othman, S.G. McFall, P.D.A. McIlroy, S.M. Nelson. *J. Chem. Soc., Dalton Trans.*, 438 (1977).
- [42] M.G.B. Drew, A.H. Bin Othman, S.M. Nelson. *J. Chem. Soc., Dalton Trans.*, 1394 (1976).